Mapping the HLA-DO/HLA-DM complex by FRET and mutagenesis

Taejin Yoon[a,1], Henriette Macmillan[a], Sarah E. Mortimer[b], Wei Jiang[a], Cornelia H. Rinderknecht[a,2], Lawrence J. Stern[b], and Elizabeth D. Mellins[a,3]

[a]Department of Pediatrics, Program in Immunology, Stanford University, Stanford, CA 94305; and [b]Department of Pathology, University of Massachusetts Medical School, Worcester, MA 01655

Edited by Daved H. Fremont, Washington University School of Medicine, St. Louis, MO, and accepted by the Editorial Board June 1, 2012 (received for review August 25, 2011)

HLA-DO (DO) is a nonclassic class II heterodimer that inhibits the action of the class II peptide exchange catalyst, HLA-DM (DM), and influences DM localization within late endosomes and exosomes. In addition, DM acts as a chaperone for DO and is required for its egress from the endoplasmic reticulum (ER). These reciprocal functions are based on direct DO/DM binding, but the topology of DO/DM complexes is not known, in part, because of technical limitations stemming from DO instability. We generated two variants of recombinant soluble DO with increased stability [zippered DOαP11A (szDOv) and chimeric sDO-Fc] and confirmed their conformational integrity and ability to inhibit DM. Notably, we found that our constructs, as well as wild-type sDO, are inhibitory in the full pH range where DM is active (4.7 to ~6.0). To probe the nature of DO/DM complexes, we used intermolecular fluorescence resonance energy transfer (FRET) and mutagenesis and identified a lateral surface spanning the α1 and α2 domains of szDO as the apparent binding site for sDM. We also analyzed several sDM mutants for binding to szDOv and susceptibility to DO inhibition. Results of these assays identified a region of DM important for interaction with DO. Collectively, our data define a putative binding surface and an overall orientation of the szDOv/sDM complex and have implications for the mechanism of DO inhibition of DM.

antigen processing | antigen presentation | MHC class II

Major histocompatibility complex (MHC) class II molecules present peptides on the antigen-presenting cell (APC) surface to sensitize $CD4^+$ lymphocytes. The class II presentation pathway is well-characterized and includes roles for three accessory molecules: invariant chain (Ii), HLA-DM (DM), and HLA-DO (DO) (1). Newly synthesized MHC class II molecules bind to Ii in the ER. A trafficking signal in the cytoplasmic domain of invariant chain directs the complex to late endosomal compartments (2, 3), called MIIC (MHC II containing compartments). The invariant chain (Ii) is proteolytically degraded in this low-pH environment, leaving a nested set of invariant chain fragments, CLIPs (class II-associated invariant chain peptides), in the class II peptide-binding groove (4). CLIP is ultimately exchanged for antigenic peptides by DM, a nonclassic MHC class II molecule, which further influences peptide selection in a process termed "peptide editing" (5–10). DM also stabilizes empty MHC class II to maintain a peptide receptive structure; otherwise, empty MHC class II proteins become peptide averse (11).

DO, another nonclassic MHC class II αβ heterodimer, first was described as an inhibitor of DM function, because overexpression of DO in human cells increased levels of CLIP-bound class II molecules (12, 13). In vitro evidence most often corroborated the view of DO as a negative modulator of DM (12, 14). Results suggesting that DO inhibition of DM is robust at early endosomal pH (6.0–6.5) and attenuated at the lower pH (4.5–5.0) of late endosomal/lysosomal MHC II containing compartments (MIICs) (14) raised the possibility that DO modifies DM-mediated peptide exchange by limiting the location of fully functional DM. This idea was consistent with evidence that DO decreased presentation of antigens taken up by fluid-phase endocytosis and enhanced BCR-mediated antigen presentation (14). DO does not unequivocally facilitate antigen presentation by all BCRs, however (15).

DO has been reported to have several functions. It mediates redistribution of DM from internal vesicles to the limiting membrane of multivesicular bodies (16) and contributes to reduced DM sorting to exosomes (17). Constitutive overexpression of DO in dendritic cells blocks disease in the nonobese diabetic (NOD) mouse model of type 1 diabetes (18). Finally, DO expression in murine B cells limits their participation in the germinal center reaction through effects on antigen presentation (19). However, the full physiological function of DO is still unclear.

In human B lymphocytes, the majority of DO is in complex with DM. DO/DM complexes are capable of egress from the ER (12, 20–22), whereas DO alone is not (23), most likely because of improper folding (24). DO instability has made functional, structural, and biochemical studies difficult. However, Thibodeau and coworkers found a point mutation (DOαP11V) that allows DO to independently egress the ER (23); this mutation is in a sequence stretch predicted by homology to influence α/β pairing. Mutation of DOαP11 allows expression in insect cells of more stable, secreted DO molecules for biochemical studies. We characterized the behavior of these molecules in DM inhibition assays, and we used in vitro fluorescence resonance energy transfer (FRET) assays and mutagenesis to study DO/DM binding orientation. Our findings have implications for the role and mechanism of action of DO.

Results

Production and Characterization of Recombinant Soluble DO. Using S2 insect cells, we expressed the luminal domains of DOα and DOβ, with additions of an αP11A mutation and C-terminal complimentary leucine zippers for increased stability, and epitope tags for purification (Fig. S1 *A* and *B*). The final yield was 0.5–1.0 mg/L insect cell supernatant, similar to MHC class II proteins such as DQ or I-A (Fig. S1*C*). Purified recombinant

Author contributions: T.Y., H.M., S.E.M., L.J.S., and E.D.M. designed research; T.Y., H.M., S.E.M., and W.J. performed research; C.H.R. contributed new reagents/analytic tools; T.Y., H.M., S.E.M., and W.J. analyzed data; and T.Y., H.M., S.E.M., L.J.S., and E.D.M. wrote the paper.

The authors declare no conflict of interest.

This article is a PNAS Direct Submission. D.H.F. is a guest editor invited by the Editorial Board.

Freely available online through the PNAS open access option.

[1]Present address: Department of Chemistry, Yonsei University, Seoul 120-749, Republic of Korea.

[2]Present address: Department of Pathology, Genentech Inc., South San Francisco, CA 94080.

[3]To whom correspondence should be addressed. E-mail: mellins@stanford.edu.

This article contains supporting information online at www.pnas.org/lookup/suppl/doi:10.1073/pnas.1113966109/-/DCSupplemental.

soluble, modified DO (hereafter "szDOv") contained a single glycan at position DOα79N (Fig. S1 *D–F*). To test whether szDOv protein was functional, we measured its capacity to inhibit sDM in endpoint class II peptide-loading assays. szDOv inhibited peptide exchange by sDM in a concentration-dependent manner, whereas two control proteins, IgG Fab (fragment antigen-binding region) and BSA, did not (Fig. 1*A*). The functionality of szDOv molecules and their conformational integrity (confirmed by precipitation with a conformation sensitive mAb; see Fig. 3*B*) supported their use in further studies. We also used S2 insect cells to prepare sDO-Fc, with the DOα and -β C termini fused to human IgG_1 Fc (crystallizable fragment) domains for stabilization, as described previously (14). DO was also expressed with DM in insect cells, and preformed DO/DM complex was purified from supernatants. The DO/DM complex was very stable, with slow dissociation over months at 4 °C (Fig. S1*G*). Following dissociation from DO, DM regained full activity in peptide association assays (Fig. S1*H*).

Soluble DO: pH-Independent Inhibition. It has been reported that the inhibition of DM by sDO-Fc is strikingly pH-dependent, with little or no inhibition at pH < 5.5 (14). Differently from this, we found that szDOv inhibits DM function across a pH range of 4.7–6.0 (Fig. 1*B*). At pH 7.0, DM peptide-loading activity was too low to evaluate inhibition, as expected based on prior data showing pH 4.5–6.0 as an optimal pH range for DM catalytic function (14, 21). The lack of pH dependence of DO activity potentially could have been attributable to the introduction of the αP11A mutation or the leucine zipper (Fig. S1*A*). To test this, we used sDO/sDM in complex or sDO-Fc (both without the αP11A mutation) and measured DM inhibition at pH 4.5–7.0. We used fluorescence polarization (FP) for real-time measurement of peptide/DR association. DO inhibition of sDM was effective at pH 4.5–6.0 using sDO-Fc (Fig. 1*C*). To verify that DO was acting on DM, and not inhibiting DR/peptide association directly, we allowed the reactions in Fig. 1*C* to come to equilibrium, because the catalytic action of DM influences the kinetics of DR/peptide interaction but not the equilibrium. At 5 d, all reactions had levels of DR1/peptide similar to that of sDR1 and peptide alone (Fig. 1*D*). Thus, DO molecules reduce the levels of complex in the shorter time frame by affecting DM catalytic action. We also studied preformed sDO/sDM complex over the same pH range (Fig. 1*C*). No increase in DM activity was observed for sDO/sDM at acidic pHs; DO inhibited DM completely whether DO was added to sDM at the beginning of the experiment or as preformed sDO/sDM. Additionally, pH does not affect the stability of preformed DO/DM complex, because complex integrity was unchanged following 4 d at pH 5 and 7 (Fig. S1*F*). Taken together, our data indicate that sDO (with or without the αP11A mutation and with or without Fc and leucine zipper) inhibits DM function in a pH-independent manner.

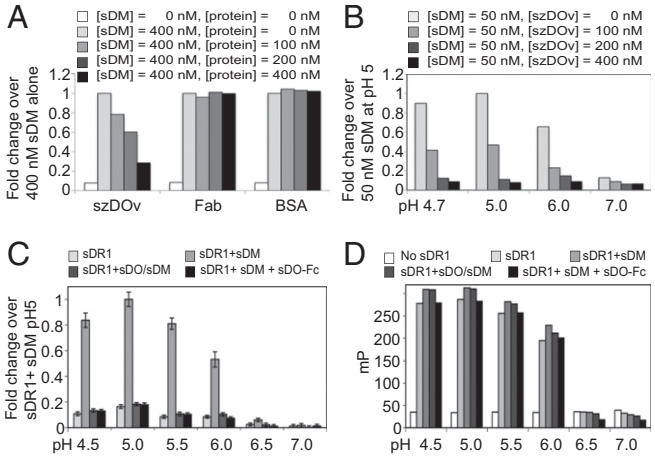

Fig. 1. pH-independent inhibition by recombinant soluble DO. (*A*) Inhibition of DM-mediated peptide loading by szDOv at pH 5. Binding of HA-biotin peptide to sDR4-CLIP with or without sDM and the indicated amounts of szDOv or control proteins was measured by capture ELISA. Data, from one of two experiments with similar results, are expressed as normalized fold change, with enhancement of peptide loading with sDM alone normalized to 1. (*B*) Inhibition of DM-mediated peptide loading by szDOv at pH 4.7–7.0. Capture ELISA data, from one of two experiments with similar results, showing loading of HA-biotin peptide on sDR4-CLIP with sDM in the presence of titrated amounts of szDOv at the indicated pH and expressed as normalized fold change, with loading by sDM alone at pH 5 normalized to 1. (*C*) Inhibition of DM-mediated peptide loading by sDO-Fc at pH 4.5–7.0. sDR1 was incubated with or without sDM, sDO-Fc, or sDO/sDM complex in citrate (pH 4.5–6), 2-(*N*-morpholino)ethanesulfonic acid (Mes) (pH 6.5), or Hepes (pH 7). Reactions were initiated by adding Alexa-488-HA peptide, and FP was measured over time. Changes in initial rate (determined from linear fits to early portions of FP change against time) were measured. Data, representative of three experiments, are fold change in initial rate of loading ± SE, relative to loading with sDM at pH 5.0. (*D*) sDO inhibition of sDM-mediated peptide loading at pH 4.5–7.0 after 5 d. FP values (mP) after 5 d of incubation of indicated proteins at indicated pH are shown.

Side-by-Side Orientation of DO/DM Complex Revealed by FRET. It has been proposed that DOαE41 and a region C terminal to DOα80 are key to DO/DM interaction (23); however, the overall structure of DO/DM complex is not well defined. We used in vitro intermolecular FRET to elucidate the binding orientation of DM and DO. FRET relies on the transfer of energy from a donor molecule (dye or fluorophore) to an acceptor molecule (dye or fluorophore); the absorption spectrum of the acceptor must overlap the fluorescence emission spectrum of the donor. The energy transfer reduces the fluorescence intensity and excited state lifetime of the donor molecule and increases the emission intensity of the acceptor molecule. The efficiency of the process depends on the inverse sixth-distance between donor and acceptor. By measuring FRET between donor fluorophores introduced at different sites on DO and an acceptor fluorophore on DM, we were able to obtain information on the relative orientation of DO and DM in the complex.

To choose sites to introduce cysteines for dye labeling, we first modeled the DO structure, using the sDR1 structure (25) as a template in the alignment mode of SWISS-MODEL (Fig. 2*A*). We identified solvent-exposed residues to minimize the effects of cysteine introduction and dye labeling on the tertiary structure of szDOv. We generated four szDOv mutants, each with a free cysteine (αA62C, αR80C, αE131C, and βS63C), and labeled them with maleimide-Cy3 as fluorescence donors (Fig. 2*A*, *Left*). The mutations are distributed over szDOv, allowing assessment of multiple regions of the molecule. Recombinant sDM has a single free cysteine at DMβ46, the mutation of which does not reduce DM function in peptide loading (26). This residue is likely to be close to both DR- and DO-binding surfaces, because an aberrant *N*-glycan at DMβN108, near sDMβC46 (Fig. 2*A*, *Right*), interferes with DM/DR and DO/DM interactions (26). Therefore, we labeled DMβC46 with maleimide-Cy5, a fluorescence acceptor. The calculated dye/protein ratios for sDM and szDOv mutants (based on the UV visible spectrum) were in the range of 0.90–0.95 dye/protein. To determine whether dye labeling disrupted DO function, we measured DM inhibition by Cy3-labeled szDOv mutants in peptide-loading assays. The labeled DO mutants exhibit concentration-dependent inhibition of DM comparable with that observed with szDOv (Fig. S2*A*). We also examined the apparent dissociation constants of unlabeled szDOv and Cy3-labeled (αE131C) szDOv with sDM using the Octet biosensor system (details in *SI Materials and Methods*). The

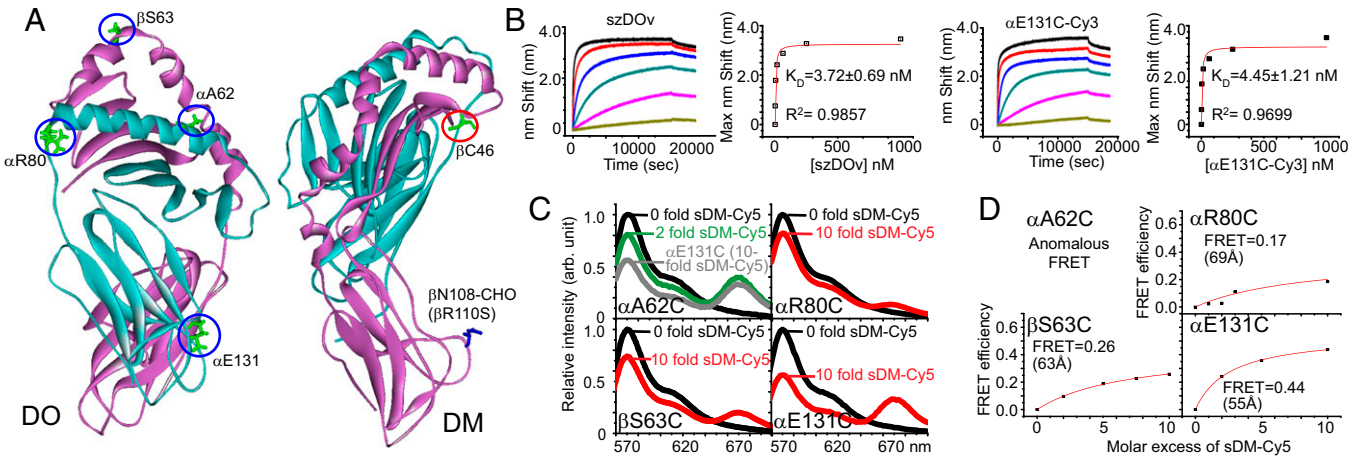

Fig. 2. In vitro FRET with szDOv and sDM. (*A*) Locations of introduced free Cys on DO (blue circles) and natural free Cys on DM (red circle). The DO structure was simulated, based on HLA-DR1 (Protein Data Bank ID code 1AQD): DOα (cyan); DOβ (purple). The DM structure was visualized using WebLab Viewer Lite V3.7: DMα (cyan); DMβ (purple). Glycan addition site (DMβN108) in mutant DMβR110S is shown. (*B*) Octet analysis of unlabeled szDOv and szDOvαE131C-Cy3 binding to immobilized sDM-biotin. Concentrations of szDOv and szDOvαE131C-Cy: 0.24 (blue), 0.98 (brown), 3.9 (pink), 15.6 (cyan), 62.5 (sky blue), 250 (red), and 1,000 nM (black). Plots of maximum wavelength (nm) shift under equilibrium binding conditions against increasing concentrations of DO were used to determine K_D. (*C*) FRET spectra of Cy3-labeled szDOv mutants and Cy5-labeled sDM. Cy3-labeled szDOvαA62C, szDOvβS63C, αR80C, and αE131C were incubated with up to 2× excess (szDOvαA62C) or up to 10× excess (others) Cy5-labeled sDM (red), as described in *SI Materials and Methods*. Spectra were obtained with buffer alone (without szDOv-Cy3), titrated with the same concentrations of sDM-Cy5, and subtracted from the corresponding FRET spectrum. (*D*) Distances between the Cy3 donor attached at different positions on szDOv (szDOvαA62C-Cy3 excluded) and the Cy5 acceptor attached at sDMβC46 were calculated: $R = R_0\ (\mathrm{FRET}^{-1} - 1)^{1/6}$, where R_0 represents 53 Å (for Cy3/Cy5). Data from one of two experiments with similar results are shown.

binding between Cy3-labeled DO and sDM ($K_D \leq 5.00$ nM) was of comparable strength to that between unlabeled szDOv and sDM (K_D~3.72 nM) (Fig. 2*B*). A total of 99% of donor dye-labeled DO molecules (100-300 nM) would theoretically be engaged in DO/DM complexes under conditions of 5× excess of acceptor dye-labeled DM molecules (500–1,500 nM). Taken together, these results showed that the Cy3-labeled DO mutants were suitable for in vitro FRET experiments.

Fluorescence emission spectra were acquired at 25 °C, with excitation at 500 nm and a 550-nm emission long-pass filter. Donor only samples (Cy3-szDOv) and an acceptor only sample (Cy5-sDM) present distinct emission maxima at 570 and 670 nm, respectively. We used a donor quenching approach, with transfer of energy from donor to acceptor reducing intensity in the donor fluorescence signal monitored at the emission maximum. Thus, donor emission decreases with increasing FRET, with the FRET efficiency differing, depending on the distance between donor (Cy3) and acceptor (Cy5).

Shown in Fig. 2*C* are the fluorescence emission spectra of DO/DM complexes with DO labeled at αR80C, αE131C, and βS63C. FRET efficiency appeared greatest when the donor was located at αE131C (at 10× Cy5-sDM: ~0.44) and least when the donor was located at αR80C (at 10× Cy5-sDM: ~0.17). In the fluorescence emission spectra of αA62C, unlike the others, donor fluorescence intensities are not proportionally decreased with increased acceptor fluorescence intensity. With the αA62C donor, acceptor fluorescence intensity at 2× Cy5-sDM (Fig. 2*C*, green) looks comparable with that of the αE131C donor at 10× Cy5-sDM (Fig. 2*C*, gray). However, donor intensity of αA62C is reduced by <50% of the reduction in intensity of αE131C, suggesting that αA62C gives anomalous FRET (see *Discussion*), and, therefore, αA62C results are excluded from distance analysis. Nonspecific FRET (either MHC class I-Cy5/sDM-Cy3 or MHC class I-Cy5/szDOv-Cy3) occurred at <10% of DO/DM FRET under the same conditions (Fig. S2*B*), arguing that DO/DM FRET results derive from the specific interaction between DO and DM.

In Fig. 2*D*, FRET efficiencies of the three informative donors are plotted as a function of fold excess of acceptor (Cy5-sDM). FRET efficiencies increased with increasing acceptor concentrations and started to saturate at 5× excess concentration of acceptor, as expected from dissociation constants. FRET efficiencies were measured in the presence of up to 10× excess acceptor, and distances (R) are derived from: $R = R_0\ (\mathrm{FRET}^{-1} - 1)^{1/6}$, where R_0 = 53 Å (for Cy3/Cy5). Collectively, the FRET results suggest that the lateral surface containing szDOvαE131C is in close proximity to sDM in the DO/DM complex.

Aberrant Glycan at DOα128 Interrupts DO/DM Interaction. To test the region around αE131C for interaction with DM, we introduced an aberrant *N*-glycan at szDOvα128 (Fig. 3*A*, mutant T128N). Glycan addition was confirmed by reduced α-chain mobility on SDS/PAGE (Fig. S1*I* and Fig. 3*B*). The intact overall structural integrity of the szDOvαT128N mutant was indicated by its recognition by a conformation-sensitive anti-DO mAb, Mags.DO5 (24), in immunoprecipitation assays (Fig. 3*B*). Inhibition of sDM by the szDOvαT128N mutant is significantly reduced in peptide-loading assays (Fig. 3*C*). Consistent with this result, the apparent K_D between sDM and szDOvαT128N is >20× higher than that of szDOv, based on equilibrium binding analysis (Fig. 3*D*). Thus, both FRET data and mutational analyses argue that the surface of szDOv containing residues αT128 and αE131 is oriented toward DM in the szDOv/sDM complex.

We also examined the effect of removing the *N*-glycan at DOαN79, using mutant szDOvαS81A (Fig. S1*I*). Immunoprecipitation of szDOvαS81A protein by Mags.DO5 (Fig. 3*B*) indicated its overall structural integrity. However, size-exclusion chromatography showed the protein was highly aggregated (Fig. S1*J*), suggesting an essential role of the glycan in preventing aggregation.

Electrostatic Interaction in the DO/DM Complex. In the DO structural model, the lateral surface we identified as the putative DM-binding region on DO includes an exposed loop with several charged residues in the α1 domain. DOαE41, located on this loop, was previously reported as important for DM binding, ER egress, and DO activity (23). In addition, the side chains of two

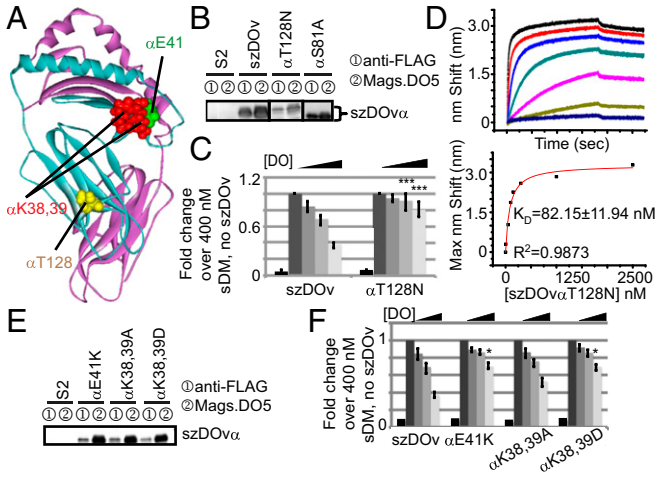

Fig. 3. Aberrant *N*-glycan at DOα128 interferes with szDOv/sDM interaction; charged residues are involved in szDOv/sDM interaction. (*A*) Model wt DO structure with DOα (cyan) and DOβ (purple) with sites chosen for mutation: szDOvαT128, positively charged szDOvαK38,39 (red), and negatively charged szDOvαE41 (green). (*B*) Structural integrity of szDOvαT128N and szDOvαS81A mutants. szDOv, szDOvαT128N, and szDOvαS81A were immunoprecipitated with indicated mAb and detected with anti-DOα rabbit polyclonal antisera. S2: untransfected S2 cells were used as a negative control. (*C*) Inhibition of DM-mediated peptide loading by szDOvαT128N. Peptide-loading data (from one of three experiments with similar results), collected as in Fig. 1*A*. Statistics were obtained by two-way ANOVA, compared with szDOv (Graphpad Prism5). ***$P < 0.001$. (*D*) Octet analysis of szDOvαT128N binding to immobilized sDM-biotin. (*Upper*) Binding of szDOvαT128N [at 5 nM (blue), 50 nM (brown), 100 nM (pink), 150 nM (cyan), 300 nM (sky blue), 1,000 nM (red), and 2,500 nM (black)]. (*Lower*) Plot of maximum wavelength (nm) shift under equilibrium binding conditions against increasing concentrations of szDOvαT128N. (*E*) Structural integrity of szDOvαE41K and szDOvαK38,39A/D mutants. szDOvαE41K and szDOvαK38,39A/D immunoprecipitated with indicated mAb and detected with anti-DOα rabbit antisera. S2: untransfected S2 cells were used as a negative control. (*F*) Inhibition of DM-mediated peptide loading by szDOv mutants. szDOvαE41K, K38,39A, and K38,39D were incubated with sDM, sDR, and peptide, as in Fig. 1*A*. Data are from one of two experiments with similar results. Statistics were obtained by two-way ANOVA, compared with szDOv. *$P < 0.05$.

lysines (DOα K38,K39) near the DOαE41 residue are predicted (in the DO model) to be solvent accessible and in the plane of the putative DM-binding face of DO (Fig. 3*A*). To evaluate the effect of these charged residues on szDOv/sDM interaction, we made a szDOvαE41K mutant, as well as two double mutants: szDOvαK38,39A and szDOvαK38,39D. These mutant molecules were conformationally intact, based on recognition by Mags. DO5 antibody (Fig. 3*E*). In comparison with szDOv, two of three mutants were less capable of inhibiting sDM in peptide-loading assays (Fig. 3*F*). szDOvαK38,39D is more defective than szDOvαK38,39A, with comparable function with szDOvαE41K in this assay. These findings argue that a lysine from αK38,K39 and the glutamic acid αE41 are among the residues involved in electrostatic interactions between szDOv and sDM and further implicate this region in szDOv binding to sDM.

Effect of Mutations in the DMβ2 Domain on Interaction with DO. Previously, we showed that full-length DMβR110S, which has an aberrant *N*-glycan at DMβN108, substantially reduces both DM/DR and DO/DM complex formation in human B cells (26). We, therefore, tested formation of szDOv/sDM complexes with soluble DM carrying this mutation (sDMβR110S). The ability of szDOv to inhibit peptide exchange by sDMβR110S could not be measured, as functional interaction with class II is severely compromised by this DM mutation (Fig. S2*C*). We measured direct binding between sDMβR110S and szDOv, using the Octet. The binding of wild-type sDM (sDMwt) to immobilized szDOv exhibits fast association and slow dissociation, whereas sDMβR110S associates more slowly and dissociates quickly (Fig. 4*A*), showing that the added glycan interferes directly or indirectly with szDOv/sDM interaction. Equilibrium binding analysis showed a reduction in the apparent K_D of interaction between sDMβR110S and szDOv compared with sDMwt (Fig. 4*B*).

We interrogated other residues in the DMβ2 domain by making additional mutations. We found that the DO inhibition capacity of sDMβH141A,S142A is significantly reduced (Fig. 4*C*), and the apparent K_D of binding to DO is modestly reduced (Fig. 4*B*). We also tested mutant sDMβE177N,I179T, which has an aberrant *N*-glycan at DMβ177 (Fig. S2*D*). This mutation did not affect the capacity of the mutant protein to be inhibited by DO (Fig. 4*C*) or to bind to DO (Fig. 4*B*), implying it is located outside the DO-binding site on DM. Our data suggest that the szDOv-binding surface on sDM includes the area around DMβN108 (the *N*-glycan location in sDMβR110S) and is influenced by the double mutation DMβH141,S142 but does not extend to sDMβE177,I179. We tested several other DM mutants located on the putative DO-binding surface and, consistent with Fig. 4 data, those show reduced interaction with DO, whereas mutants located farther from the putative DM/DO interaction surface interact well with DO (Table S1). Based on all our data, we propose an orientation of szDOv/sDM complex with the overall topology shown in Fig. 4*D*.

Discussion

DO, a nonclassic MHC class II molecule, is involved in the antigen presentation pathway as a modulator of DM (12, 13). Although data show that DO can inhibit peptide exchange catalyzed by DM, the physiological role of DO remains unknown. More detailed structural and biochemical information is likely to lead to better understanding of DO function. However, study of DO has been hindered by the instability of soluble forms of this protein. Here, we introduced a mutation at DOαP11 (P→A) that closely resembles a variant (P→V) first described by Thibodeau and coworkers (23). Removal of the proline at the DOα11 position facilitates production of more stable, recombinant, soluble DO molecules that inhibit DM in class II peptide-loading assays.

Our FRET results constrain possible orientations of DO/DM complex, and the one most consistent with the FRET data positions the lateral surface containing DOαE131 toward DM. This putative DM-binding surface on DO also is consistent with our mutagenesis results (introduction of an aberrant *N*-glycan at DOα128 and mutation of several charged residues in the α1 domain). Corroborating our findings, Thibodeau and coworkers reported that chimeric DO/DR molecules implicate DOα in interaction with DM, and they also identified DOα41 as a critical residue (23). Our data from functional assays and in vitro binding measurements of DMβ mutants suggest that a lateral face of DM (between DMβ108 and DMβ141,142) contributes to or influences the binding surface for DO.

Our overall DO/DM orientation model provides possible explanations for the anomalous FRET at αA62C. According to our model, αA62C-Cy3 is located near the interface between DO/DM. This could lead to anomalous Cy3 fluorescence enhancement or could restrict motion of the Cy3 molecule. Anomalous Cy3 fluorescence occurs when the environment surrounding the protein bound Cy3 dye becomes hydrophobic, because the fluorescence quantum yield (Φ) of Cy3 is dramatically increased with increasing viscosity (27, 28). Thus, the diminished reduction in donor fluorescence intensity of αA62C-Cy3 compared with αE131C-Cy3, despite the comparable acceptor intensities of the two Cy3 probes at 2× and 10× sDM-Cy5,

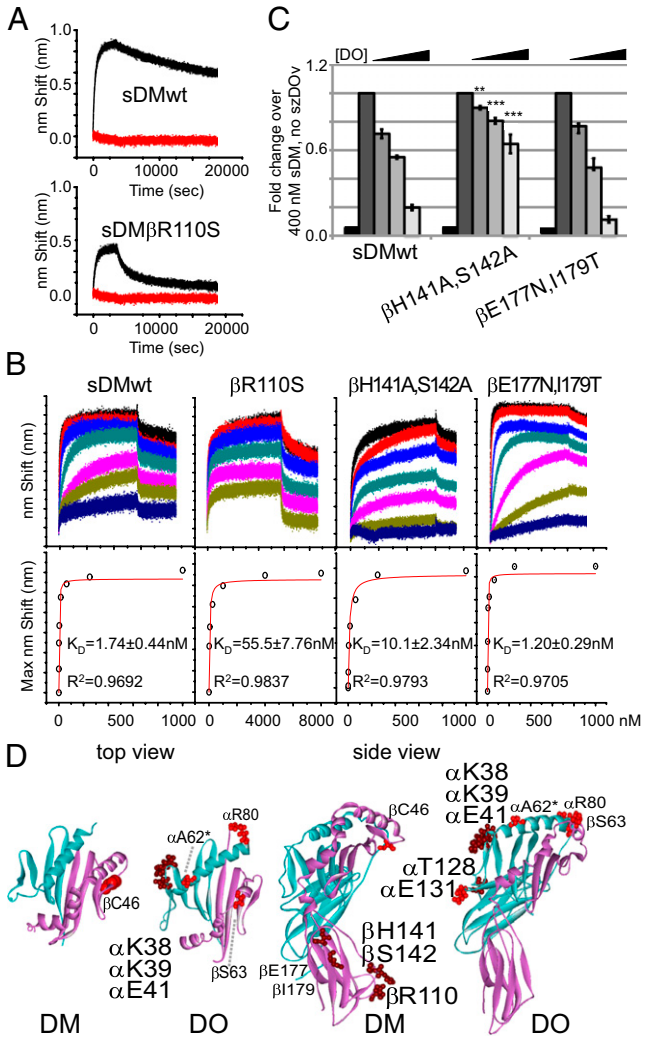

Fig. 4. Topology of DO/DM complex. (*A*) Fast dissociation of sDMβR110S from szDOv. Octet binding curves of sDMwt or sDMβR110S (both black) to immobilized szDOv-biotin. Control curves (no immobilization, no sDM) were subtracted. szDOv-biotin immobilization and no sDM is shown in red. (*B*) Octet analysis of sDMwt, sDMβR110S, sDMβH141A,S142A, and sDMβE177N, I179T binding to immobilized szDOv-biotin. (*Upper*) sDMwt, sDMβH141A, S142A, and sDMβE177N,I179T [at 0.24 nM (blue), 0.98 nM (brown), 3.9 nM (pink), 15.6 nM (cyan), 62.5 nM (sky blue), 250 nM (red), and 1,000 nM (black)] were used to determine K_D, and concentrations up to 8,000 nM sDMβR110S were used to reach saturation binding [15.6 nM (brown), 62.5 nM (pink), 250 nM (cyan), 1,000 nM (sky blue), 4,000 nM (red), and 8000 nM (black)]. (*Lower*) Plots of maximum wavelength (nm) shift under equilibrium binding conditions against increasing concentrations of sDM proteins. (*C*) Effects of DM mutations on szDOv inhibition of DM. szDOv was incubated with sDMwt, sDMβH141A,S142A, and sDMβE177N,I179T for peptide-loading assay, as in Fig. 1*A*. Background loading in the absence of sDM is in left-most bar with each set. Other bars represent data expressed as normalized fold change, with enhancement of peptide loading in the presence of each preparation of sDM alone normalized to 1. Data, from one of three experiments with similar results, are shown. Statistics were obtained by two-way ANOVA, compared with sDMwt. $^{**}P < 0.01$; $^{***}P < 0.001$. (*D*) Orientation of the szDOv/sDM complex. Top view (*Left*) and side view (*Right*) of the molecules: DMα and DOα (cyan); DMβ and DOβ (purple). Mutant residues from all experiments are indicated, with the exception of DOαS81A, which was too aggregated for study. Color code is as follows: red for residues labeled by dye addition for FRET (DO αA62, αR80, αE131, and βS63; *FRET analysis places DOαA62 closest to DM); and brown for residues altered for mutational analysis. Note: αT128N leads to glycan at αN128. βR110S leads to glycan at βN108. βE177N, I179T leads to glycan at βN177. Large font indicates residues providing data for proposed topology of the DO/DM complex; small font indicates residues that did not influence DO/DM interaction.

respectively, could reflect an increase in fluorescence quantum yield of αA62C-Cy3 in the presence of sDM. Alternatively, restricted molecular motion of the Cy3 at αA62C in the presence of sDM could induce the failure of the ideal dipole approximation, which is implicit in the Förster Eq. (29). In either case, DM itself or a conformational change in DO induced by DM influences the environment of DOαA62. Using Mags.DO5 antibody, Thibodeau and coworkers have shown that full-length DM influences the conformation of full-length DO in cells (24). The Mags.DO5 epitope is located on the DOβ chain, whereas our data suggest DM-mediated effects on DOα. The DM-mediated conformational changes in DO, including the effect on the environment of αA62 in szDOv, likely contribute to the DM chaperoning known to be required for efficient ER egress of wt DO (23).

Data from Karlsson and coworkers showed pH-dependence in DO inhibition of DM: DO efficiently blocked the peptide-editing function of DM at mild acidic pH (5.5–6.5) but not at lower pH (4.5–5.0) (14). This in vitro observation, along with several results from the H2-DO-deficient mouse (14), supported a hypothesis in which DO limits the pH range of DM function and, thereby, favors presentation of B-cell receptor (BCR)-bound antigen compared with antigen taken up by fluid-phase endocytosis. In contrast to previous results using recombinant DO, we find that several forms of recombinant, soluble DO molecules (szDOv, sDO-Fc, and sDO) inhibit peptide exchange by DM throughout the range of pH 4.5 to ∼6.0. As a consequence, DO would be expected to inhibit DM function deep into the endocytic pathway. Consistent with our findings, Denzin et al. also reported pH-independent DO inhibition with full-length DO/DM (30). A second group also observed DO inhibition of DM at pH 4.5–6.0, using DO/DM complexes from MelJuso cells (21). However, they used the term "pH-dependent" to emphasize relatively strong inhibition at pH 6 after 24 h of incubation. It is possible that the DO/DM complexes in their experiment became unstable at pH 4.5 to ∼5.0 after 24 h of incubation and that partial dissociation of DO improved DM activity under these conditions. This possibility would be consistent with our own observation that, upon prolonged storage of sDO/sDM complexes, we observed recovery of some DM activity, presumably from free DM (Fig. S1*H*).

MHC class II molecules and DO share conserved *N*-glycan motifs that differ from DM (Fig. S3). The *N*-glycans on class II are thought to play a role in proper folding of nascent molecules (31), in protease resistance (32), in facilitating optimal receptor geometry for APC/T-cell communication (33), and, most recently, in presentation of particular carbohydrate antigens (34). We found that the α1 domain *N*-glycan at szDOvαN79, near α-chain/β-chain interface and homologous to αN78 in conventional MHC class II, influences the aggregation state of the molecule (Fig. S1*J*). The homologous region of DM, which naturally lacks this *N*-glycan, has been implicated in interaction with MHC class II by mutagenesis (26). Compared with conventional class II and DO, DM has a unique *N*-glycan at DMβN92, located on the opposite side of the protein, near its α/β interface (35). This DM surface also might be prone to protein/protein interaction were it not inhibited by the presence of the glycan. Indeed, our data suggest that the homologous surfaces on MHC class II (36) and szDOv, which lack this *N*-glycan, are used for DM binding.

In our predicted overall orientation of szDOv/sDM complex, the binding surface for szDOv on sDM at least partially shares the DR-binding surface on DM strongly suggested by prior work (26, 37). Using mutant molecules for analysis, including FRET analysis after dye addition, introduces uncertainty into both the DM/DR and the DM/DO docking models. We cannot rule out subtle differences in the topology of these complexes; altering the region around DMβ141,142 confers some resistance to DO inhibition but has not been implicated in DR interaction.

Similarly, the carbohydrate adduct in mutant R110S may be mobile enough to influence contiguous, but nonidentical, sites. Nonetheless, given the strong sequence homology between DO and DR (38, 39), the most parsimonious interpretation would be that a similar, if not identical, site on DM is used to bind DO and DR and that szDOv might directly interfere with the DR/DM interaction to inhibit DM function.

In EBV-transformed human B-cell lines expressing mutant DMβ R110S (aberrant *N*-glycan at β108), levels of coimmunoprecipitated DO/DM complexes are reduced (26). Consistent with this observation, sDMβR110S has reduced apparent affinity for szDOv, arguing for similarity between the szDOv/sDM interaction and the interaction of full-length DO and DM molecules in cells. In contrast, two groups have reported a triple complex (DR/DM/DO) coimmunoprecipitated from cell lines, implying different DM-binding surfaces for DR and DO (20, 23). The discrepancy between these data and the possibility that DO and DR share a binding site may indicate that higher-order complexes combining DR/DM and DO/DM are formed in cells, perhaps with contributions from other proteins. Alternatively, there may be differences between recombinant soluble proteins and full-length proteins containing transmembrane and cytoplasmic domains. These domains may mediate intermolecular interaction between DM and DO, as shown for other membrane proteins (40). If so, these interactions influence the orientations of the intraluminal domains of full-length molecules, which may differ to some degree from the model we present here and allow triple complexes. The availability of recombinant forms of DO that can be produced efficiently should accelerate the progress in structural and kinetic studies of DO and DO/DM complexes to test our model further.

Materials and Methods

Recombinant soluble DM expression and purification was performed as described (41). Cloning, expression, and purification of recombinant soluble DO is described in *SI Materials and Methods*.

All other experimental methods are also described in *SI Materials and Methods*.

ACKNOWLEDGMENTS. We thank Drs. J. Thibodeau, L. Karlsson, and L. Denzin for reagents; Laura Su for sHLA-DR4 protein; and Guoqi Li for cys-labeled sHLA-A2. This work was supported, in part, by National Institutes of Health (NIH) Grants AI-095813 (to E.D.M.) and AI-38996 (to L.J.S.). H.M. and C.H.R. were supported by NIH Training Grant T32 AI07290 (to the Stanford Interdisciplinary Program in Immunology). H.M. and W.J. were supported by the National Center for Research Resources and the National Center for Advancing Translational Sciences, National Institutes of Health, through UL1 RR025744, and by the Lucile Packard Foundation for Children's Health, and S.E.M. was supported by NIH Grants T32 AI07349 and F32 AI072984.

1. Busch R, et al. (2005) Achieving stability through editing and chaperoning: Regulation of MHC class II peptide binding and expression. *Immunol Rev* 207:242–260.
2. Bakke O, Dobberstein B (1990) MHC class II-associated invariant chain contains a sorting signal for endosomal compartments. *Cell* 63:707–716.
3. Lotteau V, et al. (1990) Intracellular transport of class II MHC molecules directed by invariant chain. *Nature* 348:600–605.
4. Roche PA, Cresswell P (1991) Proteolysis of the class II-associated invariant chain generates a peptide binding site in intracellular HLA-DR molecules. *Proc Natl Acad Sci USA* 88:3150–3154.
5. Denzin LK, Cresswell P (1995) HLA-DM induces CLIP dissociation from MHC class II alpha beta dimers and facilitates peptide loading. *Cell* 82:155–165.
6. Morris P, et al. (1994) An essential role for HLA-DM in antigen presentation by class II major histocompatibility molecules. *Nature* 368:551–554.
7. Sloan VS, et al. (1995) Mediation by HLA-DM of dissociation of peptides from HLA-DR. *Nature* 375:802–806.
8. Weber DA, Evavold BD, Jensen PE (1996) Enhanced dissociation of HLA-DR-bound peptides in the presence of HLA-DM. *Science* 274:618–620.
9. Mosyak L, Zaller DM, Wiley DC (1998) The structure of HLA-DM, the peptide exchange catalyst that loads antigen onto class II MHC molecules during antigen presentation. *Immunity* 9:377–383.
10. Kropshofer H, et al. (1996) Editing of the HLA-DR-peptide repertoire by HLA-DM. *EMBO J* 15:6144–6154.
11. Denzin LK, Hammond C, Cresswell P (1996) HLA-DM interactions with intermediates in HLA-DR maturation and a role for HLA-DM in stabilizing empty HLA-DR molecules. *J Exp Med* 184:2153–2165.
12. Denzin LK, Sant'Angelo DB, Hammond C, Surman MJ, Cresswell P (1997) Negative regulation by HLA-DO of MHC class II-restricted antigen processing. *Science* 278: 106–109.
13. van Ham SM, et al. (1997) HLA-DO is a negative modulator of HLA-DM-mediated MHC class II peptide loading. *Curr Biol* 7:950–957.
14. Liljedahl M, et al. (1998) Altered antigen presentation in mice lacking H2-O. *Immunity* 8:233–243.
15. Alfonso C, Williams GS, Karlsson L (2003) H2-O influence on antigen presentation in H2-E-expressing mice. *Eur J Immunol* 33:2014–2021.
16. van Lith M, et al. (2001) Regulation of MHC class II antigen presentation by sorting of recycling HLA-DM/DO and class II within the multivesicular body. *J Immunol* 167: 884–892.
17. Xiu F, et al. (2011) Cutting edge: HLA-DO impairs the incorporation of HLA-DM into exosomes. *J Immunol* 187:1547–1551.
18. Yi W, et al. (2010) Targeted regulation of self-peptide presentation prevents type I diabetes in mice without disrupting general immunocompetence. *J Clin Invest* 120:1324–1336.
19. Draghi NA, Denzin LK (2010) H2-O, a MHC class II-like protein, sets a threshold for B-cell entry into germinal centers. *Proc Natl Acad Sci USA* 107:16607–16612.
20. Kropshofer H, et al. (1998) A role for HLA-DO as a co-chaperone of HLA-DM in peptide loading of MHC class II molecules. *EMBO J* 17:2971–2981.
21. van Ham M, et al. (2000) Modulation of the major histocompatibility complex class II-associated peptide repertoire by human histocompatibility leukocyte antigen (HLA)-DO. *J Exp Med* 191:1127–1136.
22. Liljedahl M, et al. (1996) HLA-DO is a lysosomal resident which requires association with HLA-DM for efficient intracellular transport. *EMBO J* 15:4817–4824.
23. Deshaies F, et al. (2005) A point mutation in the groove of HLA-DO allows egress from the endoplasmic reticulum independent of HLA-DM. *Proc Natl Acad Sci USA* 102: 6443–6448.
24. Deshaies F, et al. (2009) Evidence for a human leucocyte antigen-DM-induced structural change in human leucocyte antigen-DObeta. *Immunology* 127:408–417.
25. Stern LJ, et al. (1994) Crystal structure of the human class II MHC protein HLA-DR1 complexed with an influenza virus peptide. *Nature* 368:215–221.
26. Pashine A, et al. (2003) Interaction of HLA-DR with an acidic face of HLA-DM disrupts sequence-dependent interactions with peptides. *Immunity* 19:183–192.
27. Mujumdar RB, Ernst LA, Mujumdar SR, Lewis CJ, Waggoner AS (1993) Cyanine dye labeling reagents: Sulfoindocyanine succinimidyl esters. *Bioconjug Chem* 4:105–111.
28. Gruber HJ, et al. (2000) Anomalous fluorescence enhancement of Cy3 and cy3.5 versus anomalous fluorescence loss of Cy5 and Cy7 upon covalent linking to IgG and noncovalent binding to avidin. *Bioconjug Chem* 11:696–704.
29. Muñoz-Losa A, Curutchet C, Krueger BP, Hartsell LR, Mennucci B (2009) Fretting about FRET: Failure of the ideal dipole approximation. *Biophys J* 96:4779–4788.
30. Denzin LK, Fallas JL, Prendes M, Yi W (2005) Right place, right time, right peptide: DO keeps DM focused. *Immunol Rev* 207:279–292.
31. Määttänen P, Gehring K, Bergeron JJ, Thomas DY (2010) Protein quality control in the ER: The recognition of misfolded proteins. *Semin Cell Dev Biol* 21:500–511.
32. Van den Steen PE, Opdenakker G, Wormald MR, Dwek RA, Rudd PM (2001) Matrix remodelling enzymes, the protease cascade and glycosylation. *Biochim Biophys Acta* 1528:61–73.
33. Dustin ML, et al. (1997) Low affinity interaction of human or rat T cell adhesion molecule CD2 with its ligand aligns adhering membranes to achieve high physiological affinity. *J Biol Chem* 272:30889–30898.
34. Ryan SO, Bonomo JA, Zhao F, Cobb BA (2011) MHCII glycosylation modulates Bacteroides fragilis carbohydrate antigen presentation. *J Exp Med* 208:1041–1053.
35. van Lith M, Benham AM (2006) The DMalpha and DMbeta chain cooperate in the oxidation and folding of HLA-DM. *J Immunol* 177:5430–5439.
36. Doebele RC, Busch R, Scott HM, Pashine A, Mellins ED (2000) Determination of the HLA-DM interaction site on HLA-DR molecules. *Immunity* 13:517–527.
37. Stratikos E, Mosyak L, Zaller DM, Wiley DC (2002) Identification of the lateral interaction surfaces of human histocompatibility leukocyte antigen (HLA)-DM with HLA-DR1 by formation of tethered complexes that present enhanced HLA-DM catalysis. *J Exp Med* 196:173–183.
38. Servenius B, Rask L, Peterson PA (1987) Class II genes of the human major histocompatibility complex. The DO beta gene is a divergent member of the class II beta gene family. *J Biol Chem* 262:8759–8766.
39. Kelly AP, Monaco JJ, Cho SG, Trowsdale J (1991) A new human HLA class II-related locus, DM. *Nature* 353:571–573.
40. Matsumoto AK, et al. (1993) Functional dissection of the CD21/CD19/TAPA-1/Leu-13 complex of B lymphocytes. *J Exp Med* 178:1407–1417.
41. Busch R, Reich Z, Zaller DM, Sloan V, Mellins ED (1998) Secondary structure composition and pH-dependent conformational changes of soluble recombinant HLA-DM. *J Biol Chem* 273:27557–27564.